Wide bandgap semiconductors, nanostructures and novel devices
OTKA-NKFIH 108869
Final report

Our research is a kind of material science project with the subject of semiconductor devices. Most of the work was concentrated on GaN (and related devices. In our first work we studied GaN based metal-oxide semiconductor structures. While our partners pointed out the importance of interface charge density for the operation of such devices, we studied systematically samples in which the metal layers were plasma oxidized. We could point out that in the case of Al (AlOx) there is no amorphous interlayer to the semiconductor, which is not case however, when ZrO_2 is prepared.

(*H. Hahn, B. Pécz, A. Kovács, M. Heuken, H. Kalisch and A. Vescan: Controlling the interface charge density in GaN-based metal-oxide-semiconductor heterostructures by plasma oxidation of metal layers, J. Appl. Phys. 117 (21), (2015) 214503*)

Ni Schottky contacts to GaN were studied. The forward current-voltage characteristics of the diodes revealed a temperature dependence of both the ideality factor (n) and of the Schottky barrier height (Φ_B). The ideal value of the barrier of 1.72 eV extrapolated at n=1 was in agreement with the results obtained by capacitance-voltage measurements. A nanoscale electrical analysis performed by conductive atomic force microscopy (C-AFM) allowed to visualize the barrier height inhomogeneity and to correlate the current distribution to the surface morphology of the material. Transmission electron microscopy of the metal semiconductor interface revealed a typically flat Au/Ni bilayer structure, the Ni layer being epitaxial to GaN, with some mosaicity. The preferential current injection in the GaN areas showing hillocks, visible in the current maps, is fully consistent with the formation of a lower Schottky barrier on these surface protrusions with respect to the planar GaN regions. The results are supported by the TEM findings as well, which show beside the flat regions that in other regions along the interface with GaN, also some bumps of the Au layer have been observed on the underlying flat and homogeneous Ni layer.

G. Greco, F. Giannazzo, P. Fiorenza, S. Di Franco, A. Alberti, F. Iucolano, I. Cora, B. Pecz, F. Roccaforte, Barrier inhomogeneity of Ni Schottky contacts to bulk GaN, Phys. Stat. Solidi A, 2017, 1700613

GaN HEMTs were grown on different substrates including bulk GaN. The better epitaxial layer quality of GaN/GaN HEMTs, manifested in at least 3 orders of magnitude lower dislocation density as verified by TEM images, had a very noticeable effect on enhancing the device performance. A manuscript is submitted on this to IEEE TRANSACTION ON ELECTRON DEVICES.

While the semiconducting layers are single crystalline, the metal contacts deposited onto them are always polycrystalline. Therefore, the research (was also part of a PhD Thesis work) led by one of the senior participants (János Lábár) on the analysis of grain boundaries and on the determination of local thickness of the TEM foil was also a relevant and useful work in the present proposal. In the work precession electron diffraction too was used and methods were developed to determine how we can tilt the sample in order to get high resolution images of an appropriate grain of the polycrystalline material.

ÁK. Kiss, EF. Rauch, B. Pécz, J. Szívós and JL. Lábár: ***A Tool for Local Thickness Determination and Grain Boundary Characterization by CTEM and HRTEM Techniques***, Microscopy and Microanalysis / Volume 21 / Issue 02 / April 2015, pp 422-435

The full performance of GaN devices for high-power applications is not exploited due to the self-heating. Possible solutions are the integration of materials with high heat conductivity i.e., single crystalline diamond and graphene layers. Concerning the diamond there are two realistic solutions, one is the direct growth of GaN on diamond substrates, the another one is the growth of a polycrystalline diamond layer on the top of the device. In the latter case the grown diamond layer is always polycrystalline, which still can have high

thermal conductivity. However, the thermal transport near its nucleation site may be much lower due to the small grain size and the accumulation of defects in this region. Therefore we did study the thermal properties of polycrystalline diamond layer by Raman measurements which were correlated to TEM results. The main conclusion was that in plane thermal conductivity of the first 500 nm near the nucleation surface can be three times smaller than the in-plane thermal conductivity of the next 500 nm. These results were explained by a model taking into account the effect of the grain size on the phonon mean free path and also the energy storage in the defective region corresponding to the grain/grain interfaces. The experimental results are explained through a combined effect of the grain size and the interfaces.

(J. Anaya, S. Rossi, M. Alomari, E. Kohn, L. Tóth, B. Pécz, M. Kuball: Thermal Conductivity of Ultrathin Nano-Crystalline Diamond Films Determined by Raman Thermography Assisted by Silicon Nanowires, Appl. Phys. Lett. 106, 223101 (2015)

J. Anaya, S. Rossi, M. Alomari, E Kohn, L. Toth, B. Pecz, KD. Hobart, TJ. Anderson, TI. Feygelson, B B. Pate, M. Kuball: ***Control of the in-plane thermal conductivity of ultra-thin nanocrystalline diamond films through the grain and grain boundary properties***, Acta Materialia, Volume 103, 15 January 2016, Pages 141-152, 2016

Another possible use of diamond in the form of small single crystalline substrates (or large polycrystalline and textured wafers) is more promising. Therefore, layered structures used as HEMTs (High Electron Mobility Transistors) were grown directly onto single crystalline diamond and studied by TEM as well. In the first experiments we learned that the quality of the grown layers is strongly influenced by the formation of inversion domain boundaries during growth. An example is shown in Fig. 1. As those inversion domains are formed already on the diamond surface and appear in the thin AlN buffer layer a surface treatment of diamond was introduced and led for the growth of high quality GaN layers without the formation of inversion domains.

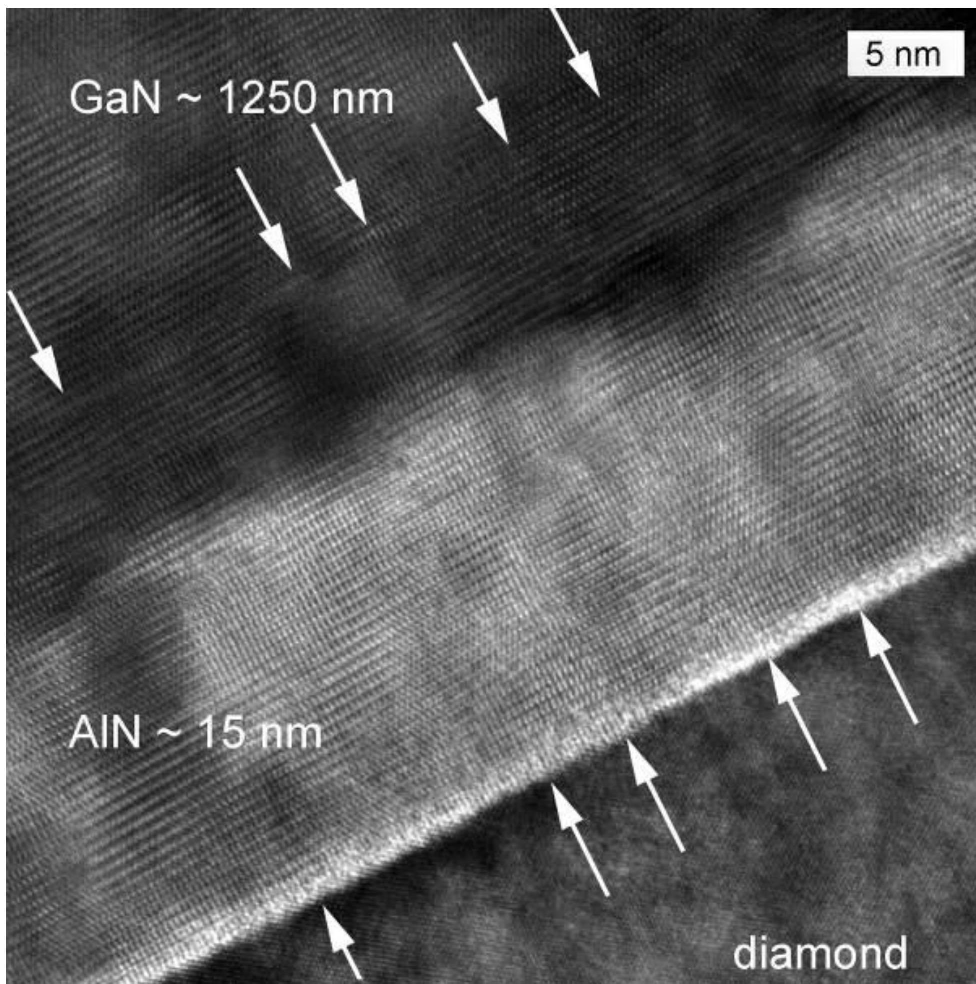

Figure 1. High-resolution TEM image of the GaN/AlN/diamond interfacial region showing a high-density of IDs (some of them are marked by arrows) in the GaN/AlN layers. The IDs formed already on the surface of diamond.

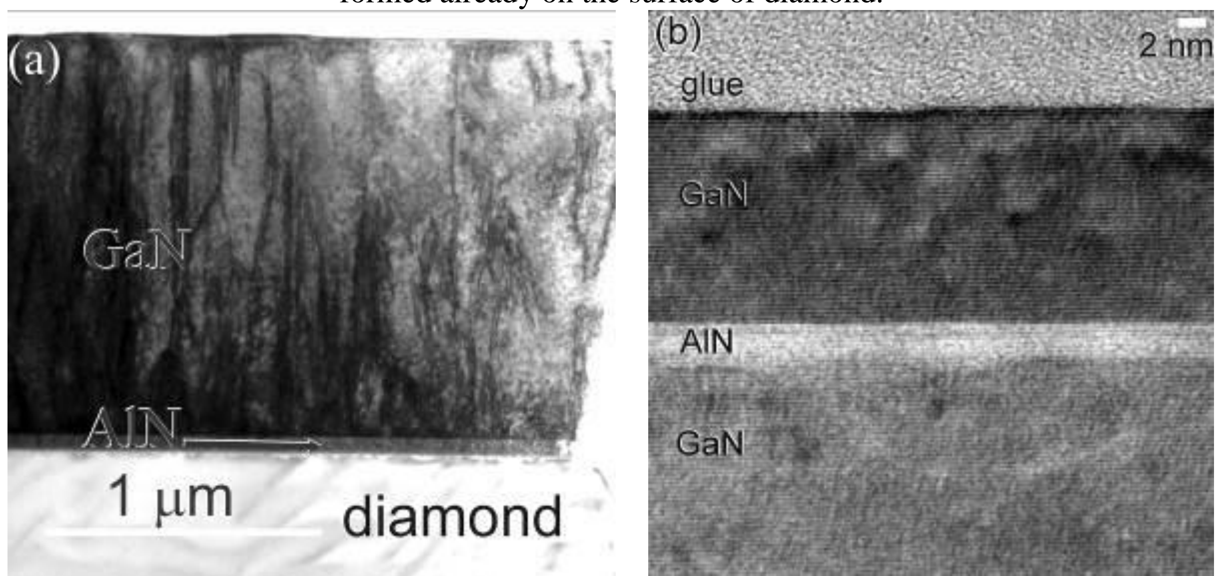

Figure 2. GaN/AlN layers grown on nitrided diamond (110) surface. (a) BF TEM image, an overview of the whole thick structure. (b) high-resolution TEM image showing active layers in the top region.

(B Pécz, L Tóth, G Tsiakatouras, A Adikimenakis, A Kovács, M Duchamp, R E Dunin-Borkowski, R Yakimova, P L Neumann, H Behmenburg, B Foltynski, C Giesen, M Heuken and A Georgakilas: GaN heterostructures with diamond and graphene, Semicond. Sci. Technol. 30 (2015) 114001 (6pp)

We know that the star material of physics, namely graphene has even higher thermal conductivity than diamond. We set up very serious plans to grow nitride layers on graphene, or somehow integrate graphene into high power devices. For this purpose it was clear for us, that instead of small flakes of graphene we need a whole wafer of Sic completely covered by graphene. This is possible to prepare on the Si face of SiC even when the graphene is not a single layer the crystallographic distances between its layers are different from those of graphite. When we do have 2-3 layers on SiC we call them FLG (Few Layers of Graphene). First we wanted to determine really how many layers we have. A new procedure was developed by us based on Auger electron spectroscopy, and by the attenuation of the signal, which could give the number of graphene layers on a large area.

L. Kotis, S. Gurban, B. Pecz, M. Menyhard, R. Yakimova: ***Determination of the thickness distribution of a graphene layer grown on a 2" SiC wafer by means of Auger electron spectroscopy depth profiling***, Applied Surface Science, 316, 301-307, 2014

Then our first experiments to grow GaN over graphene/SiC by MOCVD failed. Simply the nitride layers are not nucleated on the inert surface of graphene. Howver, we prepared a patterned graphene/SiC template by electron beam lithography and etching and the growth was repeated.

Fig. 3. a, b) Schematic figure of the patterning process and growth. c) Low magnification BF TEM overview of the heterostructure. FLG and ID indicate the few layer of graphene and inversion domain, respectively.

In regions where the AlN was nucleated over the graphene semispherical regions were observed. However, those regions were overgrown by the other ones nucleated in the 1 μm stripes of the bare SiC. The final surface after growing 2 μm thick device structure became smooth and flat.

The AlN buffer layer is rough over the graphene pads therefore it is not surprising, that the AlGaN layer grown on the buffer is also composed from hillocks. However, our electron microscopy study revealed the fact that this layer, which is a homogeneous and flat ternary layer in the control sample (without graphene) is decomposed to superlattices. The analytical investigations show, that the superlattice layers are pure AlN and GaN layers. Also the thickness of the individual AlN (1 – 1.2 nm) and GaN layers (3.6 nm) fits to the available amount of the metals in the nominal Al0.2Ga0.8N composition. The formation mechanism of

the AlN/GaN superlattices is not completely understood. However, most probably this is connected to some carbon species originating from the graphene layers and being present in the “ternary” layer.

The grown layers were tested by thermal reflectance method and the thermal resistivity is smaller above the 2 μm stripe (over graphene) than over the 1 μm stripe (no graphene). Therefore, we can say that integration of graphene into power devices is also promising for the management of self-heating problems.

A. Kovács, M. Duchamp, RE. Dunin-Borkowski, R. Yakimova, PL. Neumann, H. Behmenburg, B. Foltynski, C. Giesen, M. Heuken and B. Pécz: Graphoepitaxy of High-Quality GaN Layers on Graphene/6H–SiC, Advanced Materials Interfaces Volume 2, Issue 2, January 21, 2015. **This publication was uploaded without the impact factor. Probably worth mentioning that Advanced Materials Interfaces was launched in 2014 and received its first full Impact Factor of 4.279 in 2017.**

We have to note that the chemical nature of the graphene layers including the buffer layer on SiC was analyzed by EELS (Electron Energy Loss Spectroscopy) layer by layer. The data are in these days analyzed and compared to some DFT (Density Functional Theory) models. We expect one more publication from that. Also it is worth mentioning that we made MBE (molecular beam epitaxy) growth experiments in which it was possible to grow GaN over graphene. The grown structure was polycrystalline. However, then the experiments were concentrated to make very thin layers and try to form 2D nitrides between the graphene and SiC. The characterization of the grown structures just started.

Ga_2O_3 is a wide bandgap semiconducting oxide (~4.7 eV), promising for UV optoelectronics and power electronics. We also carried out some experiments in this system which were led by participant Ildikó Cora. Ga_2O_3 layers were grown onto (001) surface of α-Al_2O_3 by vapor phase epitaxy and were annealed at 1000 °C for 2 and 6 hours. The as-deposited layers and the two annealed samples were studied by high resolution transmission electron microscopy (TEM), X-ray diffraction (XRD) and Differential Scanning Calorimetry (DSC). The *in situ* heating was also done in TEM in order to follow the κ→β structural transformation.

Previous XRD study (F. Mezzadri, G. Calestani, F. Boschi, D. Delmonte, M. Bosi and R. Fornari. *Inorg. Chem.* 55, 12079. (2016) on the *as-deposited film* showed that these films are single crystal epitaxial layers and exhibit hexagonal $P6_3mc$ space group symmetry, characterized by partial occupation of the Ga sites, which corresponds to the ε phase, -with disordered Ga atoms in the structure. With detailed TEM studies (ED, HRTEM, STEM, simulations by JEMS) allowed to investigate the real structure of this phase at the nanoscale. The structure is ordered in 5-10 nm large (110)-twinned domains, and each domain has an orthorhombic structure with $Pna2_1$ space group symmetry, called κ-Ga_2O_3. This phase is a new polymorph among the Ga-oxides. Parallel XRD analysis carried out on thicker samples (9-10 μm) confirmed the same results, and refined structural parameters are provided.

The crystal structure of these Ga_2O_3 layers consists of an ABAC oxygen close-packed stacking, where Ga atoms in between occupy octahedral and tetrahedral sites forming two types of polyhedral layers parallel to (001). The edge-sharing octahedra and the corner-sharing tetrahedra form zig-zag ribbons along the [100] direction. Anti-phase boundaries are common inside the domains. The polar character of the structure is confirmed, in agreement with the characteristics of the $Pna2_1$ space group and explaining the ferroelectric nature.

Differential Scanning Calorimetry (DSC) up to 1100 °C was carried out on fragments of pure κ-Ga_2O_3 taken from a very thick layer[3]. This polymorph can bear long-lasting thermal treatments up to 700 °C, although some weak symptoms of lattice modifications are detected by DSC (endothermic bent) starting from about 650 °C. A complete transition to β-phase is observed for annealing temperatures ≥900 °C while at intermediate temperatures of 800 °C the films resulted very disordered and exhibited noisy diffraction spectra, with no

evident diffraction peaks of either κ or β types. The detailed structural transformation was studied by TEM during *in situ* heating (results of that are under publication).

The duration of the *ex situ* thermal treatment at 1000 °C strongly influenced the crystallinity of the samples: while for a 2 hour annealing the sample was found to be polycrystalline and strongly textured, the sample annealed for 10 hours was almost single crystalline. The sample that was *annealed ex situ for 2 hours*, consists of pure β-Ga_2O_3. The layer is polycrystalline and strongly textured: [-201] direction of each β-Ga_2O_3 crystal is perpendicular to the (001) of α-Al_2O_3. The *10 hours-long, ex situ annealed sample* is pure β-Ga_2O_3 and almost single crystalline: β-Ga_2O_3 grow onto the α-Al_2O_3 with epitaxy: (310)/[-13-1] β-Ga_2O_3 ∥ (001)/[1-10] α-Al_2O_3[3]. The upper part of the layer grows with epitaxy but with a different orientation: (310)/[-130] β-Ga_2O_3 ∥ (001)/[1-10] α-Al_2O_3.

R. Fornari, M. Pavesi, V. Montedoro, D. Klimm, F. Mezzadri, I. Cora, B. Pécz, F. Boschi, A. Parisini, A. Baraldi, C. Ferrari, E. Gombia, M. Bosi. *Acta Materialia* 140, 411-416. (2017)

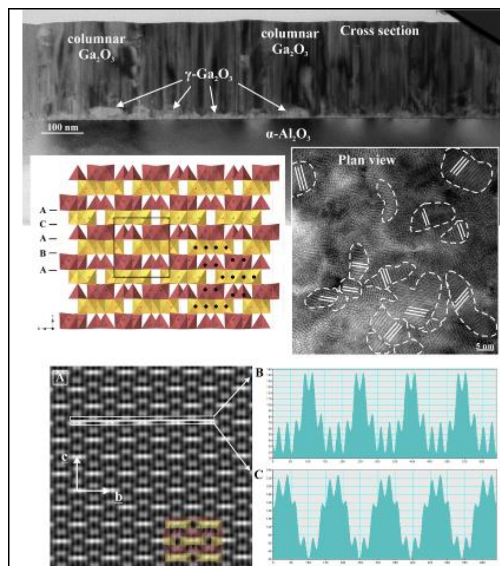

Fig.4 TEM of the as-deposited layers with the corresponding crystal structure of κ-Ga_2O_3. The structure is textured consisting of 5-10 nm large (110)-twinned orthorhombic domains. STEM image (at the bottom) with the corresponding line scans shows the Ga atoms in [100] projections.

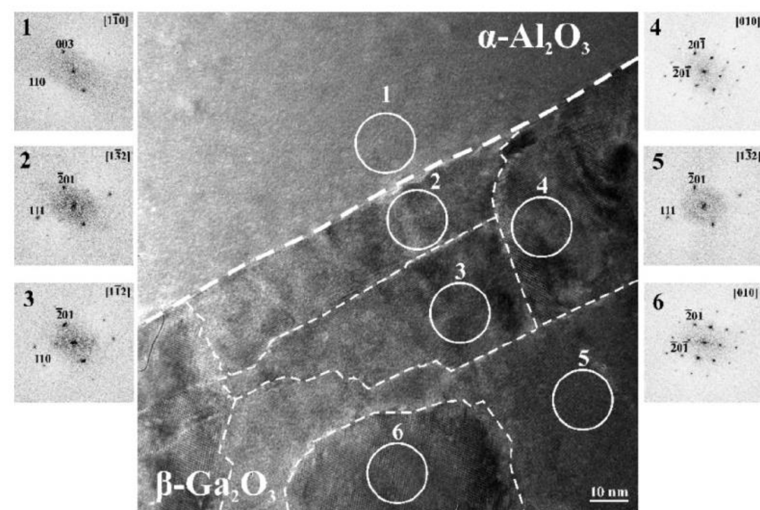

Fig.5 HRTEM images of β-Ga2O3 with the corresponding FFT patterns.

As a side activity of our project we also studied a very interesting physical phenomenon on silicon. Although metal induced crystallization of amorphous Si was a lot studied in the literature we believe that we could contribute by understanding the key factors determining the process.

Experiments were designed to characterize the resulting crystalline phases, and for studying the process in-situ by TEM.

The well known Ni-MILC process was chosen to produce crystalline Si for characterization. The process was carried out at usual and at extremely low temperatures. At low temperatures the growth of Si whiskers changes substantially: the growth direction becomes random in contrast to the [111] growth direction common in high temperature experiments. Also NiSi2 inclusions were found in the whiskers, which were characterized in detail. The inclusions

were found to be completely coherently matched to the surrounding Si phase. The interface was also determined by high resolution HAADF images. (Fig. 6)

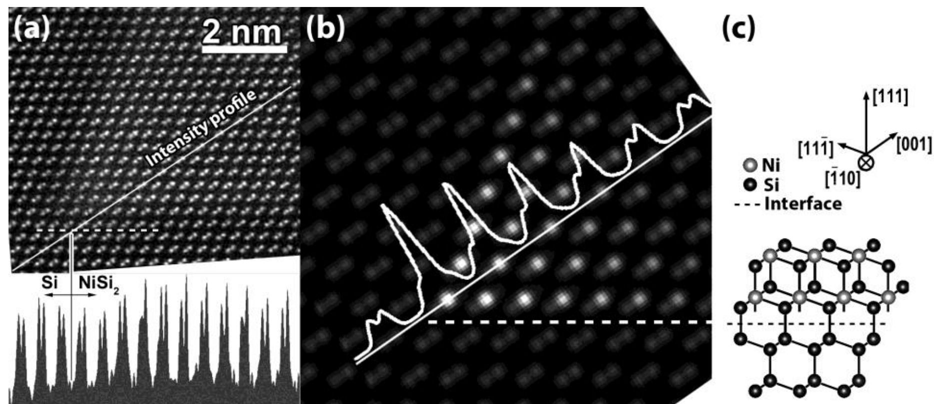

Figure 6 ***(a):*** *noise filtered STEM –HAADF image of a* $NiSi_2$ *inclusion. The sample is viewed along the [110] direction.* ***(b):*** *Simulated image of the same structure giving the same type of asymmetric dumbbells* ***(c):*** *model of the identified atomic configuration at the interface.*